EPD Congress 2016
Edited by: Antoine Allanore, Laura Bartlett, Cong Wang, Lifeng Zhang, and Jonghyun Lee
TMS (The Minerals, Metals & Materials Society), 2016

Interrupted Quasi-static and Dynamic Tensile Experiments of Fully Annealed 301 Stainless Steel

O.G. Rivera[1], Z. McClelland[2], P. Rivera-Soto[3], W.R. Whittington[4], D. Francis[4], R.D. Moser[2], P.G. Allison[1]

[1]Department of Mechanical Engineering, University of Alabama, Tuscaloosa, AL; Tuscaloosa, AL, 35487, USA
[2]Geotechnical and Structures Laboratory, US Army Engineer Research and Development Center, Vicksburg, MS; Vicksburg, MS, 39180, USA
[3]Department of Mechanical Engineering, University of Puerto Rico, Mayaguez, PR; Mayaguez, PR, 00681, USA
[4]Center for Advanced Vehicular Systems, Mississippi State University, Starkville, MS; Starkville, MS, 39762, USA

Keywords: 301 stainless steel, austenite, interrupted tensile experiment, martensite, phase transformation, split-Hopkinson

Abstract

This research examined the evolving microstructure of quasi-static and dynamically loaded fully annealed metastable 301 austenitic stainless steel (SS). Experiments were performed to an interrupted strain value of 20% and to failure using a tension Kolsky bar (1000/s) and an electromechanical load frame (0.001/s). Electron Backscatter Diffraction (EBSD) identified the microstructural evolution from the as-received condition to the 20% strain level for the high and low rate interrupted samples. This material achieved over 60% elongation to failure with increasing strength as strain rate increased, as expected. Fractography analysis using SEM showed particles in the microstructure and a ductile failure mode. The 301 SS exhibited a greater amount of phase transformation from parent austenite to α′-martensite at the dynamic strain rate when compared to the quasi-static strain rate during the interrupted experiments. This result is indicative of the increased propensity for austenite to α′-martensite phase transformations at the high strain rate.

Introduction

Austenitic alloys with metastable face centered cubic (FCC) microstructures, such as austentic stainless steel of AISI grade 301, are of great interest as a high strength and light weight material, passive safety devices and crashworthiness structure for reducing injury risks to passengers in vehicles [1] and as structural materials [2,3]. The 301 alloy exhibits excellent corrosion resistance, high energy absorption, weldability, high strength, high strain sensitivity, and high ductility when cold worked among other beneficial properties [1,4]. Table I provides the chemical composition of the 301 SS alloy. Based on this chemical composition with low Ni, Mn, and N content (all austenite / FCC stabilizers), austenitic stainless steels such as 301 exhibit low stacking fault energies (SFE) of approximately 16-18 mJ/m^2 [5]. This low SFE portends to the strong propensity of low-alloyed austenitic stainless steels to undergo austenitic to martensitic phase transformations [6]. During a cold deformation process, this material can undergo phase transformation induced plasticity (TRIP) of the face center cubic austenite; first to hexagonal closed packed ε-martensite followed by body center cubic α′-martensite [7]. This phase transformation under plastic deformation is one such intrinsic energy dissipation mechanism that is very interesting for a variety of applications requiring high strain hardening ductility with limited strain rate sensitivity.

Table I: Chemical composition of 301 SS

Carbon	Chromium	Nickel	Silicon	Manganese	Molybdenum
Max 0.12 wt%	16-18 wt%	6.5-0 wt%	<1.5 wt%	<2 wt%	<0.8 wt%

Extensive testing has been performed at quasi-static strain rates to determine flow stress, ductility, hardening behavior of metastable austenitic stainless steels and their propensity for austenite to martensite phase transformations [6,8]. These studies primarily focus on metastable stainless steel grades such as 301, 302, and 304 which have reduced Ni content. The tendancey for austenite to martensite phase transformations reduces significantly in higher alloyed grades such as 316 or nitrogen-charged (e.g., Nitronic) grades due to the increased Ni and N content, respectively. Previously, Hausild et al. [7] performed uniaxial tensile experiments at ambient temperatures on autenitic stainless steels with strain rates from 0.00005 s^{-1} to 0.05 s^{-1} and reported 912 to 866 MPa ultimate tensile strengths and 20 to 31% elongation-to-failure, respectively, with the material giving a strong strain rate dependence. The researchers observed a martensitic phase transformation after low amounts of plastic deformation.

Previous research by Lee and Lin [9] researched 304 SS in compression at different strain rates varying from 800, 2300 and 4800 s^{-1} evidenced that with higher strain rates, higher yield strength and martensite transformations occur. Research conducted by Talonen et al. [10] compared the effects of strain rates in austentic stainless steel (i.e., AISI 301LN and AISI 304) on austenite to martensite phase transformations. The strain rates studied included 3 x 10^{-4}, 10^{-2}, 10^{-1}, 1, and 200 s^{-1}, with their results also confirming that at higher strain rates, higher yield strength and martensite transformation was observed. Additional research by Lee and Lin [9] revealed that at lower strain rates, the material achieved higher strain-to-failure that is anticipated based on a reduction in yield strength and the rapid onset of martensite formation.

Additional research has studied austenitic stainless steels including varying the rate and percent reduction in area by cold rolling and its influence on grain elongation as well as annealing to induce a martensite to austenite reversion for achieving nano- / sub-micrometer grain size to improve material properties [1–3]. In order to refine the grain size, Karimi et al. [2] cold rolled a 301 stainless steel to 90% reduction in area with the reversion of martensite to austenite induced by isothermal annealing at temperatures between 600 and 900°C with varying annealing durations. Also, Misra et al. [3] using a 301 SS that had 62% cold rolled subjected to a reversion annealing of 800°C for 1 s, obtained a near complete martensite to austenite transformation with 850 MPa of yield strength and 45% of ductility. The feasibility of reversion processing and the ability to reduce grain size is promising for production of a variety of components such as thin sheets, wire, and fibers than can exhibit TRIP deformation mechanisms.

In this study, we expand on previous work by focusing on understanding austenitic to martensitic phase transformations in a metastable austentic stainless steel grade AISI 301 tested at quasi-static and dynamic strain rates. Tensile testing was performed at ambient temperature at quasi static and dynamic (1000/s) strain rates including characterization of specimens subjected to interrupted testing at 20% strain as well as experiments peformed to fracture of specimens. Post-test characterization included metallography, fractrography, crystallographic characterization using electron-backscattered diffraction (EBSD), and microhardness measurements. The goal of the research was to identify and quantify austenite to martensite phase transformations in low SFE austenitic stainless steels with the goal of their intregration into protective materials with high energy dissipation.

Materials and Methods

Microstructure characterization and tensile properties of the 301 SS material was evaluated in both the longitudinal and transverse rolling direction. A water-jet machined all the quasi-static and high rate tensile specimens to the same rectangular dog-bone geometry with a 2 mm x 2 mm cross section and a 4 mm gauge length.

Step-wise polishing for grain size and EBSD texture analysis consisted of 600 and 1200 SiC paper followed by Stuers Mol, Nap, and Chem cloths with 6 µm diamond suspension, 3 µm diamond suspension, and Struers OP-S, respectively. As a final step, an Allied High Tech vibratory polisher prepared the EBSD specimens using a cloth with 0.05 µm alumina suspension for 12 hours.

After machining, an Instron 5280 load-frame equipped with a 100 kN load cell performed ambient temperature quasi-static tensile experiments at a strain rate of 0.001/s to either fracture or an interrupted strain level of 20%. The load-frame conducted the tensile experiments in both the transverse and longitudinal plate directions to determine the mechanical behavior and identify any anisotropy in the material.

A direct tension Kolsky bar conducted the high strain rate ambient temperature experiments at a strain rate of 1000/s to either fracture or an interrupted strain value of 20%. The tension Kolsky consisted of: pulley pistons, an incident bar and a transmitted bar, where the specimen is placed in the grip of each bar as seen in Figure 1 and described previously [11–13] by the researchers. The

pulley is used to produce tension in the incident bar while the grip maintains the other end of the bar at rest. Next, the bar is released from the grip, distributing the tension along the bar. A high-speed camera correlates fracture morphology and strain data with the strain gauges on the incident and transmitted bars that are coupled with a data acquisition system to resolve the elastic waves, which provide the stress, strain, and strain rate.

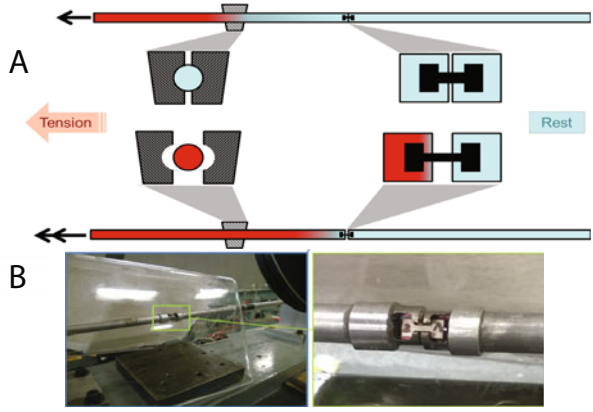

Figure 1. A) Schematic of Split-Hopkinson pressure bar. Red depicts applied tension movement and blue depicts the stationary bar. B) Tension specimen in Split-Hopkinson pressure bar grips.

Fractured specimens of both the quasi-static and high rate specimens provided fractography information by imaging in a FEI Nova NanoSEM 630 Scanning electron microscope (SEM) to identify any differences in fracture morphology observed for the different strain rates. The FEI NanoSEM 630 coupled with a Bruker e-Flash EBSD camera determined the texture analysis of the as-received untested material and interrupted quasi-static and high rate specimens. The EBSD scans obtained the phase maps on a 160x120 μm^2 area with a pixel size of 0.17 µm. The interrupted tensile experiments stopped at a strain value of 20% and coupled with the EBSD analysis evaluated the austenite to martensite transformation for the different strain rates. Interrupted high strain rate SHPB experiments were performed with the use of a connection that served as a fusible link that failed at a stress level corresponding to 20% strain.

Microhardness tests were performed to determine the effect of increased martensite composition on the hardness / strength of the material. Microhardness testing was performed using a Struers Durascan-70 microhardness indenter by indenting the as-received, quasi-static, and high rate samples in multiple locations along the middle of the gage length section of the tensile dogbone specimen.

Results and Discussion

Quasi-static tension tests were performed in both the longitudinal and transverse directions to check for anisotropic stress vs. strain behavior in the as-received 301 SS plate material. The stress-strain response of the 301SS was found to be isotropic in nature with both tested directions yielding similar responses. The 301SS tested at $0.001s^{-1}$ and room temperature exhibited an elongation to failure of approximately 70%, yield strength (YS) of 280 MPa and an ultimate tensile strength (UTS) of 900 MPa. Figure 2 depicts the quasi-static data with an optical image of the fractured specimen. Large amounts of plastic deformation and elongation of the gage section were observed with the typical cup and cone fracture morphology associated with a ductile failure mode.

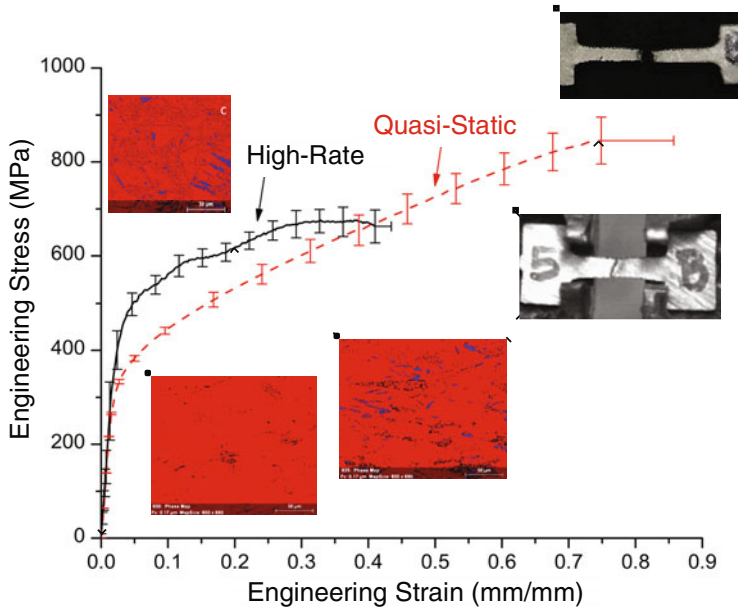

Figure 2. Comparison of the average tensile test between quasi-static and high strain rate. Red line depicts quasi-static and black line depicts high rate. Optical microscope images of the failed dogbones ductile failure for the quasi-static and mixed mode for the high rate.

High rate tensile tests were performed at a strain rate of approximately $1000/s^{-1}$ at room temperature to determine the strain rate sensitivity of the material as well as the effect strain rate has on martensitic phase transformation when compared to the quasi-static (0.001/s) tensile tests. The high rate samples exhibited a lower amount of ductility with an elongation to failure of approximately 40%, but a higher YS of 380 MPa than the quasi-static YS of 280 MPa. Both the yield stress and the stress at the equivalent 20% strain was higher for the high rate specimen. However, the ultimate tensile strength (engineering) was reduced in the specimen tested at the high

strain rate. The fractured dogbone in Figure 2 depicts an approximately 45° fracture surface that is indicative of shear bands along with ductile failure mechanisms contributing to fracture. Both the high rate and quasi-static samples displayed very similar strain hardening rates.

Fractography images captured by SEM for samples tested at the quasi-static strain rate evidenced particles in the microstructure and also the ductile failure mode evident by a dimpled fracture surface. Particles can be seen located at the bottom of voids acting as nucleation cites, followed by void growth and finally coalescence. This can be seen in Figure 3B where there are a large number of voids aligned to act as one large inclusion. The surfaces for transverse and longitudinal rolling direction samples did not present any discernable differences in the fractographic surfaces. The presence of particles is anticipated to include various impurities (carbides, sulfides, etc) in the low purity 301 SS studied.

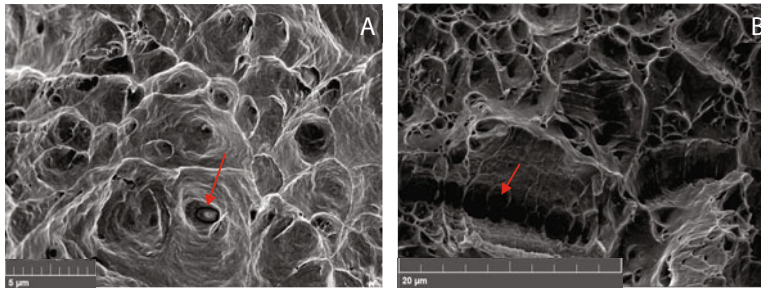

Figure 3. SE SEM fracture surface of the specimens, (A) quasi-static and (B) high strain rate

Figure 4 shows the phase maps collected from EBSD for the as-received, quasi-static, and high rate samples with the FCC austenite (γ) depicted in red and the martensite (α′) in blue. Both the quasi-static and high rate samples show long needle like structures representative of martensite produced by plastic deformation. Similar acicular needle like banding formations of martensite in partially transformed austenitic stainless steels have been reported by many other researchers [6]. As would be expected of an annealed stainless steel, the as-received sample did not contain any α′- martensite that was measureable by EBSD. The quasi-static samples microstructure contained 1.9% martensite and that of the high rate sample contained 2.8%. Additional EBSD mapping is needed to further quantify austenite to martensite transformation including studies of the failed specimens adjacent to the fracture surface. It was found that as the strain rate increased, the transformation of austenite to martensite also increased. This behavior was also reported in previous research on 304 SS and is likely associated with the uniform stress state achieved in the Kolsky bar testing as well as the rapid increase in stress throughout the specimen inhibiting localization of plasticity and in conjunction the localization of austenite to martensite phase transformations.

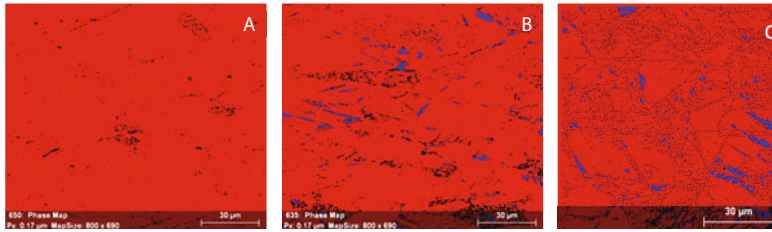

Figure 4. Microstructure phase evolution at the varying strain rates: a) material as received; b) 20% strain at 0.001/s strain rate; c) 20% strain at 1000/s strain rate. Red indicates (γ) austenite and blue indicates (α′) martensite. An increase in martensite with increasing strain rate is observed.

To confirm the microstructural trends observed in EBSD that evidenced increased martensite formation with increased strain rate, microhardness measurements were performed. Hardness is known to increase with martensite content and therefore microhardness measurements can be used to readily assess the amount and spatial distribution of martensite formation. Micro hardness tests revealed the as-received, quasi-static, and high rate samples had hardness values of 185, 277, and 293 HV, respectively. These results confirm those found in EBSD that the specimens tested at high strain rates exhibited increased martensite formation. Additional testing is needed to study the spatial distribution in martensite formation throughout the gage length of the dogbone test specimen. It is hypothesized that martensite formation will be more prevalent along the entire gage length in the high strain rate test specimen given Kolsky bar wave propagation characteristics and the delocalization of plasticity that occurs during high strain rate testing.

Conclusion

Quasi-static and high rate tension tests were conducted to determine the stress strain response and characterize the austenite to martensite transformation in specimens tested to an interrupted strain level of 20% as well as to fracture. The 301 SS specimens exhibited over 70% elongation and approximately 900 MPa tensile strength when tested at a quasi-static strain rate (0.001/!). Fracture was dominated by ductile failure mechanisms. The 301 SS specimens tested at a 1000/s strain rate exhibited an increased yield strength along with a reduction in ductility and ultimate tensile strength. These modifications in stress vs. strain behavior at high strain rates also corresponded with an increase in the formation of strain-induced α′-martensite when compared with the specimens tested at quasi-static strain rates. Relationships between martensite formation and strain rate are a result of internal stress state within specimens subjected to Kolsky testing and the delocalization of plasticity at high strain rates causing a more uniform formation of martensite throughout the specimen gage length. Additional testing to better quantify martensite formation through crystallographic or magnetic properties measurements along with the spatial distribution of martensite measured by microhardness or nanoindentation mapping is needed.

Acknowledgements

Funding for this work was provided by the 6.1 Military Engineering Basic Research Program of the US Army Engineer Research and Development Center. Permission to publish was granted by Director, Geotechnical and Structures Laboratory, US Army Engineer Research and Development Center.

References

[1] M. Eskandari, A. Najafizadeh, A. Kermanpur, M. Karimi, Mater. Des. 30 (2009) 3869–3872.
[2] M. Karimi, a. Najafizadeh, a. Kermanpur, M. Eskandari, Mater. Charact. 60 (2009) 1220–1223.
[3] R.D.K. Misra, B.R. Kumar, M. Somani, P. Karjalainen, Scr. Mater. 59 (2008) 79–82.
[4] AK Steel, Prod. Data Bullletin (n.d.).
[5] R.E. Schramm, R.P. Reed, Metall. Trans. A 6 (1975) 1345–1351.
[6] J. Dash, H.M. Otter, Acta Metall. 11 (1963).
[7] P. Haušild, V. Davydov, J. Drahokoupil, M. Landa, P. Pilvin, Mater. Des. 31 (2010) 1821–1827.
[8] M. Milad, N. Zreiba, F. Elhalouani, C. Baradai, J. Mater. Process. Technol. 203 (2008) 80–85.
[9] W.-S. Lee, C.-F. Lin, Mater. Sci. Eng. A 308 (2001) 124–135.
[10] J. Talonen, H. Hänninen, P. Nenonen, G. Pape, Metall. Mater. Trans. A 36 (2005) 421–432.
[11] W.R. Whittington, a. L. Oppedal, S. Turnage, Y. Hammi, H. Rhee, P.G. Allison, C.K. Crane, M.F. Horstemeyer, Mater. Sci. Eng. A 594 (2014) 82–88.
[12] P.G. Allison, M.F. Horstemeyer, Y. Hammi, H.R. Brown, M.T. Tucker, Y.K. Hwang, Mater. Sci. Eng. A 529 (2011) 335–344.
[13] O.L. Rodriguez, P.G. Allison, W.R. Whittington, D.K. Francis, O.G. Rivera, K. Chou, X. Gong, T.M. Butler, J.F. Burroughs, Mater. Sci. Eng. A 641 (2015) 323–327.